

## BIOMECHANICAL UNDERSTANDING OF BLOW-OUT FRACTURES: A FINITE ELEMENT STUDY

Abdul-karim Khalil\* | Khodor Khafif\*\* | Amjad Atieh\*\*\*

### Abstract

Blow-out fractures are one of the most common fractures in maxillofacial trauma. Two mechanisms are thought to cause these fractures, the buckling mechanism and hydraulic mechanism.

This study aims to compare between the two mechanisms in terms of intensity and extension using the finite elements method.

Three-dimensional model was generated using computed tomography data of young male patient. Virtual loads were applied on the infra-orbital rim and the eyeball separately.

Von Mises stress and equivalent elastic strain were examined in each simulation.

The simulation predicted fractures on the infra-orbital rim and orbital floor when simulating the buckling mechanism, and on the orbital floor and mesial wall when simulating the hydraulic mechanism.

Biomechanical studies are essential in understanding maxillofacial fractures mechanisms. Our results ascertained and confirmed what is seen clinically and explained the two mechanisms of blow-out fractures.

**Keywords:** Orbit - blow-out fractures - finite element analysis - hydraulic mechanism - buckling mechanism.

IAJD 2019;10(2):60-66.

## COMPRÉHENSION BIOMÉCANIQUE DES FRACTURES DU PLANCHER DE L'ORBITE: ÉTUDE PAR ÉLÉMENTS FINIS.

### Résumé

*Les fractures du plancher de l'orbite de type (blow-out) sont des fractures courantes dans les traumatismes maxillo-faciaux. On pense qu'il existe deux mécanismes à l'origine de ces fractures, le mécanisme de flambement et le mécanisme hydraulique.*

*Cette étude vise à comparer les deux mécanismes en termes d'intensité et d'extension à l'aide de la méthode des éléments finis.*

*Un modèle tridimensionnel a été généré à l'aide des données de tomographie par ordinateur d'un jeune patient. Des charges virtuelles ont été appliquées sur le globe oculaire pour simuler le mécanisme hydraulique et sur le bord infra-orbitaire pour simuler le mécanisme de flambement. L'énergie de déformation et le stress de Von Mises ont été examinés dans chaque simulation.*

*La simulation a prédit des fractures au niveau du rebord infra-orbitaire et du plancher orbitaire lors de la simulation du mécanisme de flambement, ainsi que sur la paroi mésiale et le plancher de l'orbite lors de la simulation du mécanisme hydraulique.*

*Les études biomécaniques sont essentielles pour comprendre les mécanismes des fractures maxillo-faciales. Nos résultats ont permis de vérifier et de confirmer les observations cliniques et d'expliquer les deux mécanismes de fracture par éclatement.*

**Mots-clés:** orbite – fractures - analyse par éléments finis - mécanisme hydraulique - mécanisme de flambement.

IAJD 2019;10(2):60-66.

\* Dpt of Oral and Maxillofacial Surgery,  
Faculty of Dentistry,  
Tishreen University, Lattakia, Syria  
Karimplus60@gmail.com

\*\* Lecturer,  
Dpt of Design and production,  
Faculty of Mechanical & Electrical  
Engineering, Tishreen University,  
Lattakia, Syria

\*\*\* PhD Student,  
Dpt of Oral and Maxillofacial Surgery,  
Faculty of Dentistry,  
Tishreen University, Lattakia, Syria

## Introduction

Blow-out fractures are one of the most common facial fractures seen in maxillofacial surgery, so it is important to understand their mechanisms for effective prevention and treatment [1, 2]. Several studies have been conducted to illustrate the mechanisms of blow-out fractures [3, 4]. Two mechanisms are thought to cause blow-out fractures, the hydraulic mechanism and the buckling mechanism.

The hydraulic mechanism suggests that increased pressure within the components of the orbit causes the fragile walls of the orbit to fracture [5], while the buckling mechanism suggests that the walls of the orbit bend in response to trauma and then fracture [6].

The first to introduce the buckling mechanism was Le Fort in 1901. This mechanism was defined as the transfer of force across the bone from the infra-orbital rim to the orbital floor [7]. This theory was widely accepted as well as the hydraulic mechanism as a cause of blow-out fractures [8]. Several experimental studies in literature support the buckling mechanism [3-6, 9-11]. They simulated the fractures of the orbit by dropping a pre-measured weight or hitting the bony orbit using hammer.

Fujino et. al. [6] conducted experiments using skulls without the eyes and the contents of the orbit, they hit the skulls on the infra-orbital rim, thus eliminating the influence of the hydraulic mechanism, focusing on the buckling mechanism [9]. Waterhouse et. al. also developed a new device that allows a point-based impact to a specific area of the orbit [4]. Using this device and striking the eyeball or the infra-orbital rim on skulls individually, they illustrated the fracture patterns for both mechanisms.

It is logical that in vivo research is the best approach for understanding the biomechanical behavior of the maxillofacial complex, but the ethical considerations in experimenting with humans and the technical difficulties

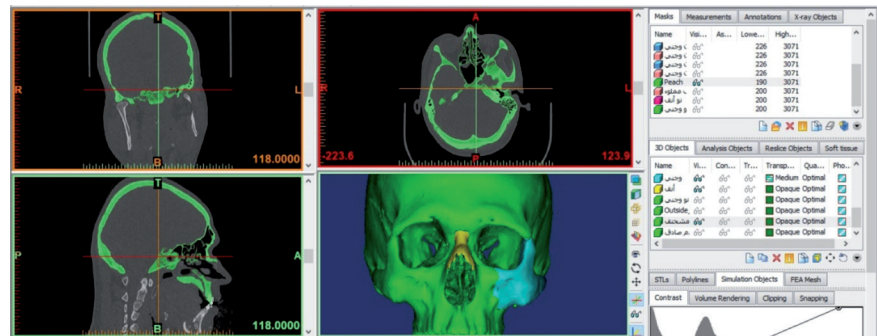


Fig. 1: MIMICS software, used in 3D model construction.

in placing multiple gauges on this complex limit the ability to achieve satisfactory results [12].

The use of preserved human skulls to conduct in vitro studies can provide good understanding of the biomechanics of this complex. However, the difficulty in obtaining enough samples of well-preserved skulls, the complexities in measurement of loads and stresses and the difficulty in placing different types of gauges to measure different stress types limit the ability to achieve comprehensive results [13].

Finite element models showed a high degree of success in predicting the biomechanical behavior of skeletal bones such as long bones and iliac bone [14, 15]. The finite element method is a numerical method that offers approximate solutions for complex problems. This technique relies on replacement of complicated differential equations of irregular shapes with an extensive system of algebraic equations, which represent small geometric entities that can be solved by a computer [16]. In this method, the studied structure is modeled into a mesh of tetrahedral elements (the finite elements) that are connected together with nodes. The physical properties of these elements are assigned, a number of these elements are constrained and known forces are applied and the stresses and strains are calculated at each node and in each element [17]. Bone fractures occur on the surface that is subjected to stress greater than the permissible stress value of the bone.

Simulation of blow-out fractures using finite elements method can help to understand their biomechanical behavior and improves current surgical treatment protocols. The aim of this study is to compare between the orbital fractures resulting from impact on the infra-orbital rim (buckling mechanism) and fractures resulting from direct impact to the eyeball (hydraulic mechanism) in terms of intensity and extension using the finite elements method.

## Materials and methods

Finite element method was used to investigate the two theories of blow-out fractures.

### Work steps:

1. Dicom files were obtained from computed tomography (Siemens SOMATOM, 0.6mm thickness) of 35 years old male patient, as most of those exposed to facial trauma are males from this age range [18]. The data was obtained from Radiology Department at Tishreen University Hospital, Lattakia, Syria.
2. No ethical consideration was needed. Patient approval was taken to use his CT data in this study.
3. Dicom files were Imported into MIMICS software (Materialise, inc, Belgium) [19] to:
  - Isolate the bone using Tresholding algorithm.

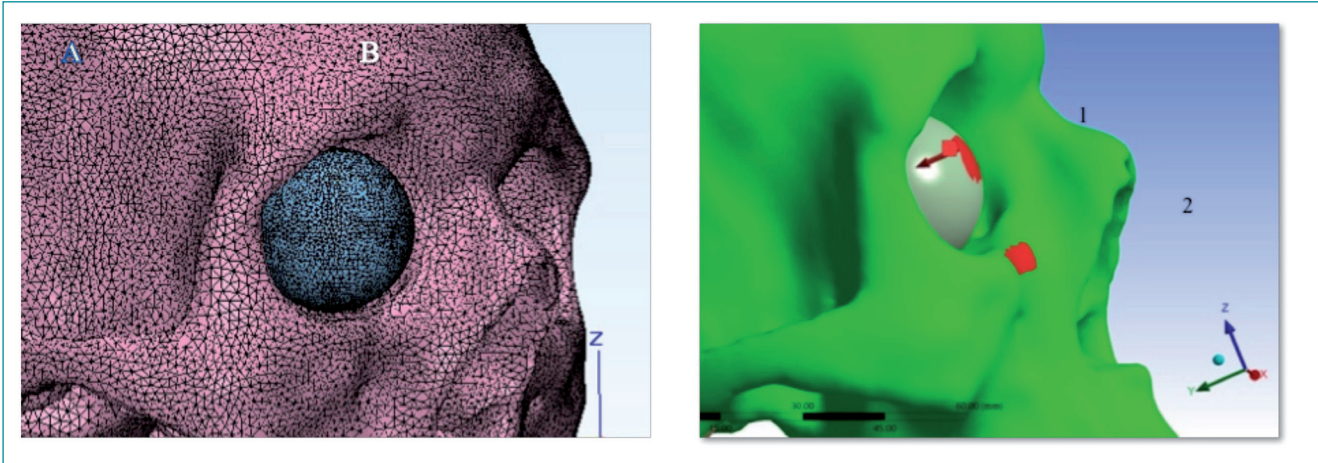


Fig. 2: (A): 3-MATIC software, meshing the skull surface and virtual eyeball. (B): ANSYS software, marked sites on virtual eyeball and infraorbital rim where loads will be applied.

- Build a 3D model of the skull (Fig. 1).
  - Emit the mandible from the skull because our study focuses on the orbit only.
4. 3D model was exported to 3-MATIC software (Materialise, inc, Belgium) [20] to:
- Design a sphere that touches the inner walls of the orbit thus simulating the eye.
  - Mesh the surface, where it was divided into triangular elements connected to each other by nodes (Fig. 2, A).
  - Create volume mesh based on the surface mesh (dividing the body into tetrahedral elements that are connected with nodes) which was about 560000 elements.
  - Convert 4-noded tetrahedral elements into 10-noded tetrahedral elements which are better for analysis results accuracy.
5. 3-MATIC file (.cdb) was exported to ANSYS software 18.1 (Ansys inc, USA) [21] for finite element analysis as follows:
- The areas where the loads will be applied were marked (on the infra-orbital rim and the center of the virtual eyeball) as shown in (Fig.2, B).
  - Mark areas to be constrained (the two occipital condyles of the skull).
  - Material properties were assigned for both the skull bone and the eyeball: density, Young's modulus and Poisson ratio, as follows:
    - Young modulus was calculated based on density values according to Morgan approach 2003 [22], where each element of the volumetric mesh is assigned with individual values for physical properties, including both Young modulus and density values with the help of APDL Script in the Ansys software. Poisson ratio was assigned to 0.3 according to Huskes study in 1987 [23].
    - The virtual eyeball was assigned to Young modulus of Water at 2,000 MPa [24] due to its high-water content, and density of water is known to be 997 kg/m<sup>3</sup>. Poisson ratio of the entire eyeball was obtained from medical literature at 0.47 [25].
    - The contact surface between skull and virtual eyeball was modeled using coulomb friction model. The coefficient of friction for this contact was defined with 0.3 [26].
  - 6. We chose two study designs to simulate what is seen clinically:
    - Apply force to the virtual eyeball simulating the hydraulic mechanism.
    - Apply force to the infra-orbital rim simulating the buckling mechanism.
  - 7. Virtual static loads were applied in the two designs along Y axis which is perpendicular to the surface on which the load was applied. The load was gradually increased by 100N at a time until we reached Von Mises stress value of about 153 MPa. We assumed that the Von Mises stress above 153 MPa was the criteria of failure for skull bones according to Nagasao et. al. study 2006 [27], where this stress value is when the bone change from the elastic phase to the plastic phase and then begins to fail (fracture).
  - 8. The skull was fixed at the occipital condyles in all degrees of freedom.
  - 9. When the stresses exceeded the value of 153Mpa, the causal load was recorded in each design.
  - 10. The skull sutures were not specifically modeled because the assignment of material properties of each region takes these sutures into account by attributing specific values for each region.
- We chose to study von Mises stress which can predict body failure accurately, and equivalent elas-

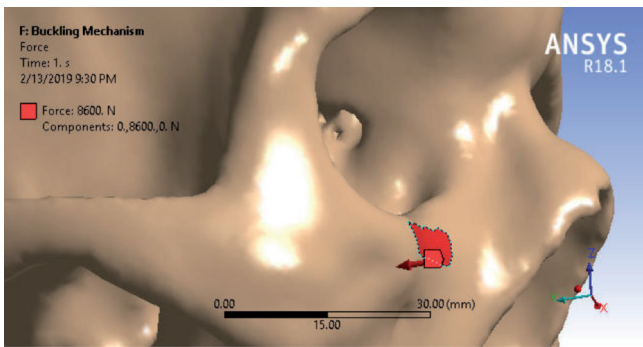


Fig. 3: ANSYS, marked area on the infra-orbital rim and the force applied (8600N).

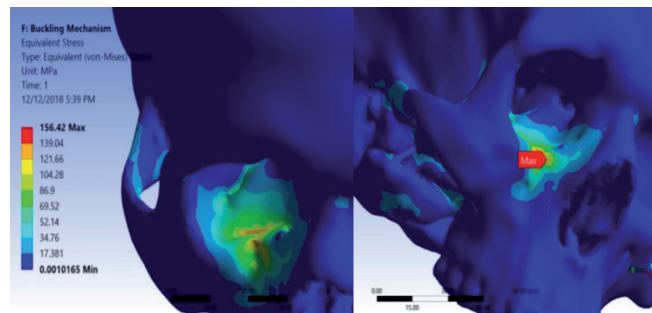


Fig. 4: Distribution of Von Mises stress when simulating the buckling mechanism. Theoretically, fracture is expected to occur in areas where stress value exceeds the 153 MPa threshold which is plotted in red color in this simulation and the highest stress region were labeled with (max) sign.

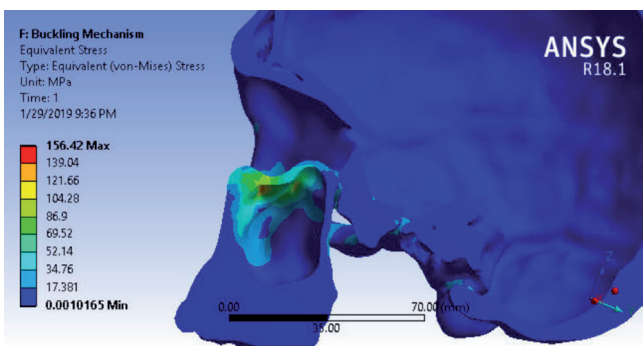


Fig. 5: A sagittal cross section in the skull under load at the infra-orbital rim area. This section shows stresses extend to front and mesial sinus wall.

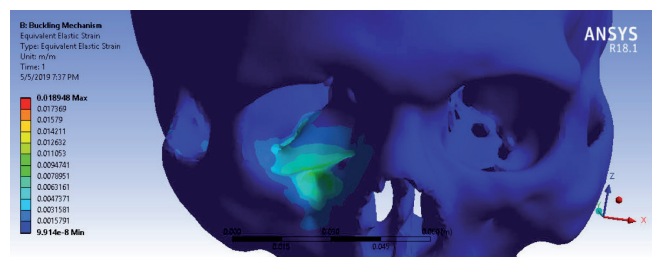


Fig. 6: Equivalent elastic strain distribution on the infra-orbital rim showing a locally confined area around impact site where strain (deformation) was concentrated.

tic strain which represent the deformation (mm) in the material (bone/eye) caused by the load applied.

## Results

We were able to generate a detailed model of the skull of young male with a dense volume mesh of about 560000 finite elements. Using such dense model, the details of the midface, orbit and surrounding bones were represented in this study. The two mechanisms of blow-out fractures were simulated and compared in term of intensity and extension.

Von Mises stress, and equivalent elastic strain were evaluated. Results were plotted as color spectrum ranged from blue to red, where red indicates the highest value of calculated stress or strain.

First simulation: load on the infra-orbital rim.

We conducted a virtual simulation of an impact on the infra-orbital rim to study the buckling mechanism and the resultant orbital fractures.

We gradually increased the load until we got a stress value higher than the 153 MPa criteria. We found a maximum stress value of 156 MPa when applying a force of 8600 N at the infra-orbital rim along the Y-axis on the 1 cm<sup>2</sup> pre-defined area (Fig. 3).

We found concentration of stresses in the infra-orbital rim and orbital floor, where red spots indicate that the stresses are approaching the threshold of 153 MPa, which means we can predict a fracture in these two regions (Fig. 4).

Stress spread to the front and mesial sinus wall and skull base without reaching the 153 MPa threshold

as shown in cross section in the skull (Fig. 5).

When evaluating equivalent elastic strain, concentrations of strain were observed on infra orbital rim as shown on (Fig. 6), which indicates that the bone in this area absorbed the load.

### Second simulation: load on virtual eyeball.

We conducted a virtual simulation of an impact on the eyeball to study the hydraulic mechanism and the resultant orbital fractures.

We found a maximum Von Mises stress value of 155 MPa when applying a force of 7200 N on the eyeball along the Y axis on the 1cm<sup>2</sup> predefined areas (Fig. 7).

The analysis results revealed concentration of stresses in the orbital floor and the medial wall of the orbit (Fig. 8), showing concentrations of red



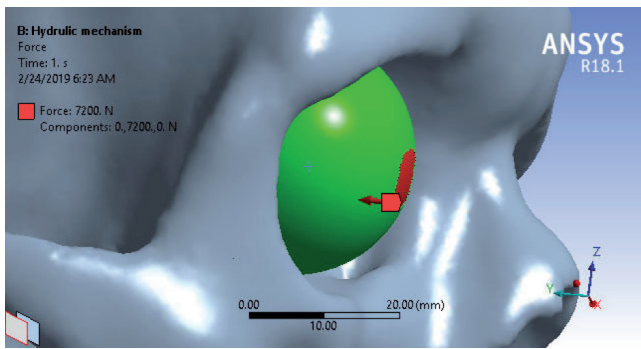


Fig. 7: Marked area on the virtual eyeball and the force applied (7200N).

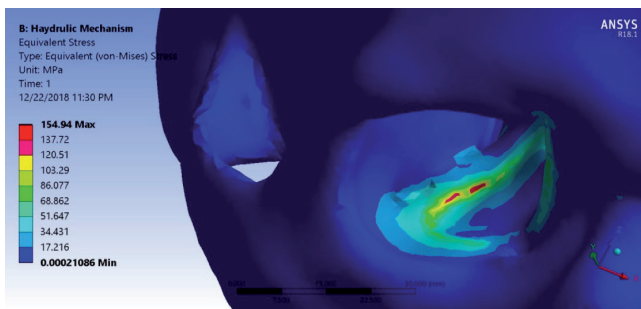


Fig. 8: Hydraulic mechanism simulation: Distribution of von Mises stresses up to the 153 MPa threshold where the highest concentrations of stresses at orbital floor.

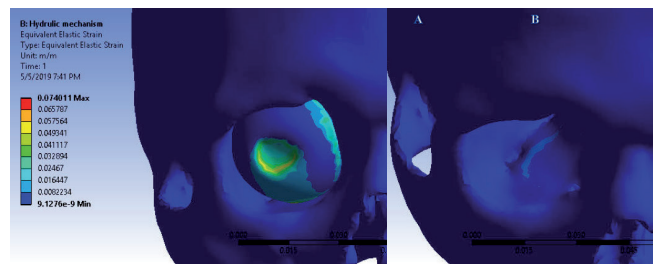


Fig. 9: Equivalent elastic strain distribution on the eyeball (A), and orbital floor (B) when simulating the hydraulic mechanism. Highest elastic strain (deformation) was at the eyeball.

color at the orbital floor indicating that the stresses are approaching or exceeding the 153 MPa threshold, which means we can predict a fracture in this area.

Simulation revealed that most of the strain was concentrated in the eyeball, and little on orbital floor (Fig. 9). These findings suggest that the deformation of the eyeball absorbed most of the load applied.

## Discussion

The main idea of finite elements analysis is to describe the mechanical behavior of any object by dividing it into small parts and calculating the loads and stresses affecting each part solely. The finite element method has been used in scientific research for decades and is used for biomechanical studies of several organs such as bone [28], teeth [29], skin [30], vessels [31], and blood flow [32]. Blow-out fractures occur when the traumatic force affects the orbit area in the event of traffic

accidents, personal violence, and war injuries [33, 34]. Most existing studies on blow-out fractures used experimental methods like, hitting skulls with pre-measured objects [3-6, 9-11]. However; it is difficult to maintain the continuity of the experiment conditions because these conditions are easily affected by differences in: impact points, angle of the skull or skull stabilization. To solve this problem, we simulated the skull and performed a finite element analysis on it. Since it is possible to reproduce the experiment accurately by this method, it is appropriate to use finite element analysis for this study. We were able to repeat the simulation many times until we reached the stress threshold described by Nagassao [27], which is difficult to achieve using experimental methods.

Several studies have been conducted to illustrate orbital fractures using the finite element method. Nagasao et al. [27] placed 1085 points on the surface of a dry skull and then the coordinates of the marking points

were measured using a 3D scanner and then he built a 3D model based on the data from the scanner. Our model was based on data from a computed tomography of a 35-year-old male, producing a model that represents the skull well and simulates real anatomy, including the variable bone thickness.

Our study results showed that we need a larger force to fracture the orbit when applied to the infra-orbital rim than when applied to the eyeball. This can be explained by the fact that the relatively thick bone in the infra-orbital rim dampens and disperses the stresses more effectively than the eyeball, which transfer the force in greater efficiency to the relatively thin walls of orbit. As shown in figure 6, equivalent strain was the highest on the infra-orbital rim.

The detailed finite element model used for simulation (560k elements), the relatively good resolution of bony structures, and material assignment of each region ensure good representation of the skull both anatomically

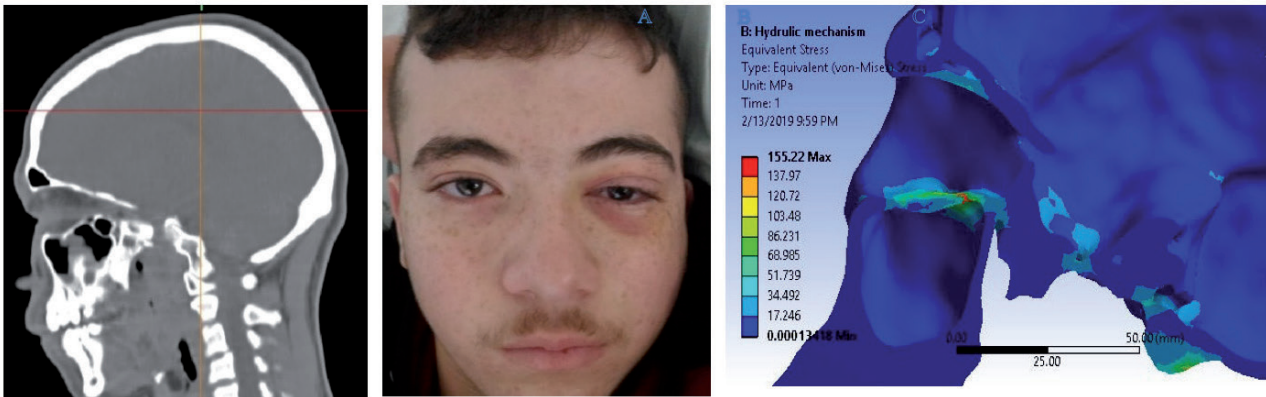


Fig. 10: A 19-years old patient with blow-out fracture caused by personal violence, CT scan revealed an orbital floor fracture which is corresponded to our results as shown in the sagittal cross section.

and biomechanically. This good representation ensures good and reliable results.

In first simulation: the results simulated the buckling mechanism of the orbital fractures, and revealed a fracture in the infra-orbital rim and the orbital floor, which corresponds to the model found by Waterhouse and colleagues in 1999 [4], where they hit the infra-orbital rim experimentally. The fracture pattern also corresponds with the results of Nagasao study [27] where they found that fracture occurs in the weakest parts of orbit (orbital floor). In second simulation: the results simulated the hydraulic mechanism of orbital fractures, where we found concentration of stresses on the walls of orbit with the greatest at the orbital floor, Low stresses have spread to all the walls of the orbit, but they can not necessarily cause a fracture. However, increasing the force applied can cause the other walls of other orbit to fracture, which simulates a blow-out fracture in both the mesial wall and orbital

floor, which is often seen clinically in patients with this type of trauma (Fig. 10).

The results of the study can be used to predict the risk of blow-out fractures during clinical trials. When doctors examine patients suspected of having blow-out fractures, the determination of the exact cause can be achieved. The presence of edema or hematoma in the sclera or cornea indicates that the eyeball has received the force and that the hydraulic mechanism is involved. In contrast, a hematoma or edema in the lower eyelid or irregularity at infra-orbital rim indicates that the buckling mechanism is involved.

Modeling orbital contents (muscles and fat) and the soft tissue covering the bone will increase the accuracy of the results. This consideration should be taken into account in the future when better computer capabilities and more advanced computed tomography is available, allowing the modeling of the orbital contents separately .

## Conclusion

Biomechanical studies are essential to understand maxillofacial fractures mechanisms. Our results ascertained and confirmed what is seen clinically and explained the mechanisms of blow-out fractures. The results of this study can help to optimize fracture therapies and improve their outcomes. These simulations help in investigating trauma scenarios and mechanism which could be useful in forensic sciences.

## Conflict of interest

The authors have no proprietary, financial, professional, or other personal relationships with any product, other people, or service that could be construed as inappropriately influencing their work in this manuscript.

## References

1. Kaufman Y, Stal D and Cole P. Orbitozygomatic fracture management. *Plast Reconstr Surg.* 2008;121:1370-1374.
2. Suzuki H, Furukawa M and Takahashi E. Barotraumatic blowout fracture of the orbit. *Auris Nasus Larynx.* 2001;28:257-259.
3. Green Jr RP et al. Forces necessary to fracture the orbital floor. *Ophthal Plast Reconstr Surg.* 1990;6:211-217.
4. Waterhouse N, Lyne N and Urdang M. An investigation into the mechanism of orbital blowout fractures. *Br J Plast Surg.* 1999;52:607-612.
5. Rhee JS et al. Orbital blowout fractures: experimental evidence for the pure hydraulic theory. *Arch Facial Plast Surg.* 2002;4:98-101.
6. Fujino T, Sugimoto O and Tajima C. Mechanism of orbital blow out fracture: II. Analysis by high speed camera in two dimensional eye model. *Keio J. Med.* 1974;23:115.
7. Le Fort R. Etude expérimentale sur les fractures de la mâchoire supérieure. *Rev. Chir. Paris.* 1901;23:208.
8. Smith B and Regan W. Blow-out fracture of the orbit Mechanism and correlation of internal orbital fracture. *Am.J. Ophthalmol.* 1957;44:733.
9. Tajima S, Fujino T and Oshiro T. Mechanism of orbital blowout fracture: I. Stress coat test. *Keio J. Med.* 1974;23:71.
10. Ahmad F et al. Strain gauge biomechanical evaluation of forces in orbital floor fractures. *Br J Plast Surg.* 2003;56:3-9.
11. Ahmad F et al. Buckling and hydraulic mechanisms in orbital blowout fractures: fact or fiction? *J Craniofac Surg.* 2006;17:438-441.
12. Ross C F and Hylander W L. In vivo and in vitro bone strain in the owl monkey circumorbital region and the function of the postorbital septum. *Am J Phys Anthropol.* 1996;101:183-215.
13. Provatidis C et al. validated finite element method model for a human skull and related craniofacial effects during rapid maxillary expansion. *Proc Inst Mech Eng H.* 2006;220:897-907.
14. Ramos A and Simoes J A. Tetrahedral versus hexahedral finite elements in numerical modelling of the proximal femur. *Med Eng Phys.* 2006;28:916-924.
15. Anderson A E, et al. Subject-specific finite element model of the pelvis: Development, validation and sensitivity studies. *J Biomech Eng.* 2005;127:364-373.
16. Ottosen N S and Petersson H. Introduction to the Finite Element Method. New York : Prentice Hall, 1992.
17. Maloul A and et al. Biomechanical Characterization of Complex Thin Bone structures in The Human Craniofacial Skeleton. University of Toronto : s.n., 2012, PHD.
18. Elhammali N, Bremerich A and Rustemeyer J. Demographical and clinical aspects of sports-related maxillofacial and skull base fractures in hospitalized patients. *Int J Oral Maxillofac Surg.* 2010;39:857-862.
19. Materialise MIMICS. [Online] 10 2016. <http://biomedical.materialise.com/mimics>.
20. Materialise 3-matic. [Online] Matrialise, 2016. <http://biomedical.materialise.com/3-matic>.
21. ANSYS. [Online] ANSYS, 2016. <http://www.ansys.com/>.
22. Morgan E F, Bayraktar H H and Keaveny T M. trabecular bone modulus-density relationships depend on anatomic site. *J Biomech.* 2003;36:897-904.
23. Huiskes R. Finite element analysis of acetabular reconstruction. *Acta Orthop.* 1987;57:620-625.
24. Sigloch H. Technische Fluidmechanik. Berlin : Springer-Verlag, 2009.
25. Uchio E, Ohno S and Kudoh J. Simulation model of an eyeball based on finite element analysis on a supercomputer. *Br J Ophthalmol.* 1999;83:1106-1111.
26. Tensi H M, Gese H and Ascherl R. Non-linear three-dimensional finite element analysis of a cementless hip endoprosthesis. *Proc Inst Mech Eng H.* 1989;203:215-222.
27. Nagasao T and Miyamoto J. The effect of striking angle on the buckling mechanism in blowout fracture. *Plast Reconstr Surg.* 2006;117:2373-2381.
28. Remmler D, Olson L and Ekstrom R. Pre-surgical CT/FEA for craniofacial distraction: I. Methodology, development, and validation of the cranial finite element model. *Med Eng Phys.* 1998;20:607-619.
29. Nagasao T, Kobayashi M and Tsuchiya Y. Finite element analysis of the stresses around fixtures in various reconstructed mandibular models. *J Craniomaxillofac Surg.* 2002;30:170-177.
30. Mizunuma M, Yanai A and Tsutsumi S. Can dog-ear formation be decreased when an S-shaped skin resection is used instead of a spindle skin? A three-dimensional analysis of skin surgery techniques using the finite element method. *Plast Reconstr Surg.* 2000;109:763.
31. Beller C J, Labrosse M R and Thubrikar M J. Role of aortic root motion in the pathogenesis of aortic dissection. *Circulation.* 2004;109:763.
32. Shojima M, Oshima M and Takagi K. Magnitude and role of wall shear stress on cerebral aneurysm: computational fluid dynamic study of 20 middle cerebral artery aneurysms. *Stroke.* 2004;35:2500-2505.
33. Shere J L et al. An analysis of 3599 midfacial and 1141 orbital blowout fractures among 4426 United States Army Soldiers, 1980–200. *Otolaryngol Head Neck Surg.* 2004;130:164-170.
34. Agir H, Ustundag E and Iscen D. Bilateral isolated orbital blowout fractures among terrorist bombing victims. A very rare entity. *J Plast Reconstr Aesthet Surg.* 2006;59:306-307.